

Cite this: DOI: 10.1039/xxxxxxxxxx

Twist–bend nematic phases of bent–shaped biaxial molecules

Wojciech Tomczyk*, Grzegorz Pająk** and Lech Longa***

 Received Date
 Accepted Date

DOI: 10.1039/xxxxxxxxxx

www.rsc.org/journalname

How change in molecular structure can affect relative stability and structural properties of the twist–bend nematic phase (N_{TB})? Here we extend the mean–field model¹ for bent–shaped achiral molecules, to study the influence of arm molecular biaxiality and the value of molecule’s bend angle on relative stability of N_{TB} . In particular we show that by controlling biaxiality of molecule’s arms up to four ordered phases can become stable. They involve locally uniaxial and biaxial variants of N_{TB} , together with the uniaxial and the biaxial nematic phases. However, the V–shaped molecule show stronger ability to form stable N_{TB} than a biaxial nematic phase, where the latter phase appears in the phase diagram only for bend angles greater than 140° and for large biaxiality of the two arms.

1 Introduction

One of the most surprising recent discovery in the field of soft matter physics is the identification of a new nematic phase, known as the nematic twist–bend phase (N_{TB})^{2–4}. This phase is stabilized as a result of spontaneous chiral symmetry breaking in liquid crystalline systems composed of achiral bent–core⁵, dimeric⁶ and trimeric⁷ mesogens. The director in N_{TB} forms a conical helix with nanoscale periodicity, while molecular achirality implies that coexisting domains of opposite chirality are formed. Up to now, only some characteristic features of this elusive phase are known, like *e.g.*, tilt angle and the pitch length or values of elastic constants in the vicinity of the uniaxial nematic (N_U) – N_{TB} phase transition^{8–13}. Experiments show that the N_{TB} phase usually occurs within the stability regime of N_U ¹⁴, but for some compounds a direct transition between N_{TB} and the isotropic phase (Iso) has also been found¹⁵. Although mechanism leading to long–range chiral order of N_{TB} is to a large extent unknown, the issue of stable, modulated nematic phases has been addressed theoretically in a series of papers^{16–27}.

Meyer^{25,26} and subsequently Dozov²⁷ have shown that flexopolarization can be the driving force leading to twist–bend and splay–bend distortions of the director field. Lorman and Mettout^{28,29}, suggested that the formation of the N_{TB} , and other unconventional periodic structures, can be facilitated by the shape of bent–core molecules, which seems to be in line with experimental results^{14,30} and computer simulations^{3,22,31,32}.

Out of alternative theoretical approaches undertaken to tackle the nature of N_{TB} we will focus on a generic, mean–field model introduced by Greco, Luckhurst and Ferrarini (GLF)¹. In the GLF model N_{TB} is treated as an inhomogeneous and *locally* uniaxial heliconical periodic distortion of the nematic phase, characterized at each point by the single local director $\hat{\mathbf{n}}(\mathbf{r}) \equiv \hat{\mathbf{n}}(z)$ ^{1,27} (see Figure 1):

$$\hat{\mathbf{n}}(z) = [-\sin(\theta)\sin(\phi), \sin(\theta)\cos(\phi), \cos(\theta)], \quad (1)$$

where θ is the conical angle and $\phi = kz = \frac{2\pi}{p}z$ with wave vector $\mathbf{k} = k\hat{\mathbf{z}}$ ($k = \pm \frac{2\pi}{p}$) and with period p of the phase. The wave vector, being parallel to the average direction of the main director over one period p : $\mathbf{k} \parallel \langle \hat{\mathbf{n}} \rangle_p$, can be identified with an effective optical axis^{16,17,19}.

Heliconical precession is assumed arbitrarily to take place around the $\hat{\mathbf{z}}$ –axis of the laboratory system of frame. The helix of N_{TB} can be right–handed or left–handed, depending on the sign of k , and both of these mono–domains have the same free energy. Moreover, a rigid, biaxial bent–core molecule is represented by two mesogenic arms of cylindrical symmetry, each assumed to align preferentially to $\hat{\mathbf{n}}(z)$. The latter is taken at the position of the midpoint of the arm. Only N_{TB} , N_U and the isotropic liquid can be stabilized by the GLF model.

The effective mean–field potential acting on molecular arms is defined by the well–known Maier–Saupe P_2 potential, with P_2 being the second Legendre polynomial. Despite its simplicity the GLF model correctly predicts N_U to N_{TB} and Iso to N_{TB} phase transitions, weak temperature dependence of the pitch and consistent description of elastic properties of the N_{TB} . Tailoring molecules with particular shapes and interactions, it seems interesting to study extensions of the GLF model to molecules of more complex

Marian Smoluchowski Institute of Physics, Department of Statistical Physics, Jagiellonian University, prof. S. Łojasiewicza 11, 30-348 Kraków, Poland.;

*E-mail: wojciech.tomczyk@doctoral.uj.edu.pl

**E-mail: grzegorz@th.if.uj.edu.pl

***E-mail: lech.longa@uj.edu.pl

structure.

While there are many paths that can be followed, one obvious observation is that bent-shaped molecules, including the famous N_{TB} -forming compound CB7CB, can acquire biaxiality not only due to their average "V" shape, but also as a result of biaxiality of molecule's arms and conformational degrees of freedom^{33,34}. Importantly, they can form a stable biaxial nematic phase^{35–37}, and, hence, this structure should be included into theoretical analysis as a possible competitor of N_{TB} .

Biaxiality is also regarded as a key factor to get spontaneous chiral symmetry breaking from first principles³⁸. These symmetry arguments are supported by recent phenomenological analysis of modulated nematic structures using generalized Landau–de Gennes–Ginzburg theory, where the key ingredients were couplings between the alignment tensor field and steric polarization²⁴. In this theory the N_{TB} phase, described by a locally uniaxial distortion of the director field, appears less stable than its locally biaxial counterpart, *i.e.* where full spectrum of distortions of the alignment tensor are taken into account. Following this direction we extend the GLF model to study the effect of molecular biaxiality of bent-core molecules on stability of N_{TB} and of competing nematic phases, including biaxial one. For this purpose we replace the local twist–bend spatial modulation of the director field (1) by its biaxial counterpart, given by the local alignment tensor. We also let the molecular biaxiality of banana-shaped molecules to enter not only through their "V" shape but also through biaxiality of molecular arms. This extension allows to treat arm molecular biaxiality as an extra parameter characterizing bent-shaped molecules, in addition to the bend angle.

This paper is organized as follows. In the second Section we define extension of the GLF model and underline its important features. Next we interpret acquired results in the third Section. The last Section is devoted to a short discussion.

2 The model

2.1 Molecular geometry and director profiles

Here we keep parametrization¹ for molecular reference frames, where two mesogenic arms A and B, each of length L , are joined at the bend angle χ (Figure 1). At the midpoint of each arm a molecular basis is placed. The unit vector $\hat{\mathbf{w}}$ at the center (C) of the particle describes molecular C_2 axis. In line with the present model of the N_{TB} phase^{1,27} we generalize the local uniaxial *ansatz*, represented by the main director (1), by its local biaxial counterpart (kept from the start in the variational *ansatz* for local environment of the molecule). That is, we assume two other directors to follow the precession of $\hat{\mathbf{n}}(z)$ (Figure 1):

$$\hat{\mathbf{m}}(z) = [\cos(\phi), \sin(\phi), 0], \quad (2)$$

$$\hat{\mathbf{l}}(z) \equiv \hat{\mathbf{n}}(z) \times \hat{\mathbf{m}}(z) = [-\cos(\theta)\sin(\phi), \cos(\theta)\cos(\phi), -\sin(\theta)]. \quad (3)$$

As for GLF the parametrization (1-3) permits the N_{TB} phase for $0^\circ < \theta < 90^\circ$ and finite pitch p , with wave vector \mathbf{k} being parallel to the $\hat{\mathbf{z}}$ axis.

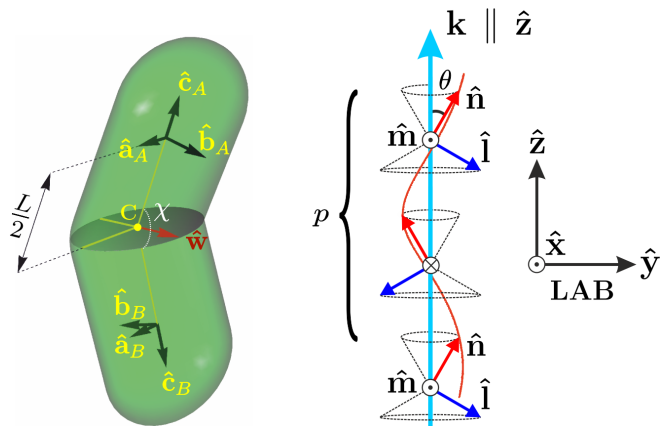


Fig. 1 (Color online) On the left side is a schematic representation of extended biaxial model for bent-shaped molecule with both arms of equal length L . Molecular basis for arm A is given by orthonormal tripod of vectors $\Omega_A = \{\hat{\mathbf{a}}_A, \hat{\mathbf{b}}_A, \hat{\mathbf{c}}_A\}$, and for arm B by $\Omega_B = \{\hat{\mathbf{a}}_B, \hat{\mathbf{b}}_B, \hat{\mathbf{c}}_B\}$. C_2 axis of molecule is along unit vector $\hat{\mathbf{w}}$, attached at point C. Bend angle is denoted as χ . Sketch on the right-hand side of the figure shows a visualization of local directors used in the mean-field *ansatz* for N_{TB} structure, where local director basis $\{\hat{\mathbf{n}}, \hat{\mathbf{m}}, \hat{\mathbf{l}}\}$ on each arm precesses on a cone of pitch p and tilt angle θ between primary director $\hat{\mathbf{n}}$ and wave vector \mathbf{k} .

2.2 Formulation of the mean-field potential

In the first step we extend the GLF model by introducing molecular biaxiality on both of the arms of the molecule, which is achieved via second-rank, 3×3 , symmetric and traceless tensor \mathbf{Q} . The basis of the \mathbf{Q} tensors, defined with respect to the orthonormal right-handed tripod, say $\{\hat{\mathbf{x}}, \hat{\mathbf{y}}, \hat{\mathbf{z}}\}$, comprises both uniaxial \mathbf{Q}_U and biaxial \mathbf{Q}_B parts, given in the general form as³⁹:

$$\mathbf{Q}_U(\hat{\mathbf{z}}) \stackrel{\text{def}}{=} \frac{1}{\sqrt{6}}(3\hat{\mathbf{z}} \otimes \hat{\mathbf{z}} - \mathcal{I}), \quad (4)$$

$$\mathbf{Q}_B(\hat{\mathbf{x}}, \hat{\mathbf{y}}) \stackrel{\text{def}}{=} \frac{1}{\sqrt{2}}(\hat{\mathbf{x}} \otimes \hat{\mathbf{x}} - \hat{\mathbf{y}} \otimes \hat{\mathbf{y}}), \quad (5)$$

where \otimes denotes the tensor product and \mathcal{I} is the identity matrix. Taking linear combination of \mathbf{Q}_U and \mathbf{Q}_B the molecular tensors for each arm are now defined as:

$$\mathbf{Q}(\Omega_i) \stackrel{\text{def}}{=} \mathbf{Q}_U(\hat{\mathbf{c}}_i) + \lambda\sqrt{2}\mathbf{Q}_B(\hat{\mathbf{a}}_i, \hat{\mathbf{b}}_i), \quad (6)$$

where the λ parameter is a measure of the arm's biaxiality and where $\Omega_i = \{\hat{\mathbf{a}}_i, \hat{\mathbf{b}}_i, \hat{\mathbf{c}}_i\}$ is the molecular right-handed tripod attached to arm $i = A, B$ (Figure 1). Please observe that the GLF model¹ corresponds to $\lambda = 0$. In addition we should mention that the $\mathbf{Q}(\Omega_i)$ tensor can be linked to the diagonal elements of molecular polarizability tensor⁴⁰ for the arm i .

The next step is decomposition of the tensor $\langle \mathbf{Q}(\Omega_j) \rangle \stackrel{\text{def}}{=} \bar{\mathbf{Q}}(\hat{\mathbf{n}}(R_j), \hat{\mathbf{m}}(R_j), \hat{\mathbf{l}}(R_j)) \equiv \bar{\mathbf{Q}}(R_j)$, which is obtained from Eq. (6) by performing thermodynamic average. In the basis (4,5) it reads:

$$\begin{aligned} \bar{\mathbf{Q}}(R_j) &= \bar{\mathbf{Q}}_U(R_j) + \bar{\mathbf{Q}}_B(R_j) \\ &= q_0\mathbf{Q}_U(\hat{\mathbf{n}}(R_j)) + q_2\mathbf{Q}_B(\hat{\mathbf{m}}(R_j), \hat{\mathbf{l}}(R_j)), \end{aligned} \quad (7)$$

where $\{\hat{\mathbf{n}}(R_j), \hat{\mathbf{m}}(R_j), \hat{\mathbf{l}}(R_j)\}$ are the three local directors at the position R_j of the midpoint of the j -th arm ($j = A, B$), and where

q_0 and q_2 are the uniaxial and biaxial order parameters of an arm, respectively. The local directors are identified with eigenvectors of the $\bar{\mathbf{Q}}$ tensor and the corresponding eigenvalues⁴¹ are given by $\mu_m = -q_0/\sqrt{6} + q_2/\sqrt{2}$, $\mu_l = -q_0/\sqrt{6} - q_2/\sqrt{2}$ and $\mu_n = -\mu_m - \mu_l = \sqrt{2/3}q_0$. From this perspective the locally isotropic phase is met when all three eigenvalues of $\bar{\mathbf{Q}}$ are equal, which means $\bar{\mathbf{Q}} \equiv \mathbf{0}$. For the locally $D_{\infty h}$ -symmetric uniaxial states two out of three eigenvalues of $\bar{\mathbf{Q}}$ are equal, i.e., $q_0 \neq 0$, $q_2 = 0$ or $q_0 \neq 0$, $q_2 = \sqrt{3}q_0$ or $q_0 \neq 0$, $q_2 = -\sqrt{3}q_0$. In the general case, $\bar{\mathbf{Q}}$ has three different real eigenvalues that correspond to the local, D_{2h} -symmetric biaxial state.

Finally, we can write down a full mean-field potential as a natural extension of that proposed by GLF¹. It reads

$$H_{\text{MF}}(\Omega) = -\varepsilon \text{Tr}[\mathbf{Q}(\Omega_A) \cdot \bar{\mathbf{Q}}(R_A) + \mathbf{Q}(\Omega_B) \cdot \bar{\mathbf{Q}}(R_B)], \quad (8)$$

where ε is the coupling constant, \cdot denotes matrix multiplication and Ω stands for the molecular orientation expressed in terms of Euler angles that define this orientation in a local $\{\hat{\mathbf{n}}, \hat{\mathbf{m}}, \hat{\mathbf{l}}\}$ frame. The corresponding mean-field equilibrium free energy per particle resulting from orientational degrees of freedom is given by:

$$f = q_0^2 + q_2^2 - t^* \ln Z, \quad (9)$$

where Z is the orientational one-particle partition function:

$$Z = \int e^{-H_{\text{MF}}(\Omega)/t^*} d\Omega, \quad (10)$$

and where $t^* \stackrel{\text{def}}{=} k_B T / \varepsilon$ is the (dimensionless) reduced temperature. Orientational averages of any one-particle quantity $X(\Omega)$ are calculated in a standard way as:

$$\langle X(\Omega) \rangle = \frac{1}{Z} \int X(\Omega) e^{-H_{\text{MF}}(\Omega)/t^*} d\Omega. \quad (11)$$

Taking parametric form (1–3, 7) of the alignment tensor $\bar{\mathbf{Q}}$ the equilibrium structure can be obtained by minimization of the free energy, Eq. (9), with respect to the order parameters q_0 and q_2 and the "local environment" parameters θ and p . The former ones are given self-consistently by:

$$q_n = \frac{1}{2} \langle q_n(\{R_A\}, \Omega_A) + q_n(\{R_B\}, \Omega_B) \rangle, \quad n = 0, 2, \quad (12)$$

where the orientational averaging applies to the symmetry adapted functions which are given in a typical form^{39,41}:

$$q_0(\{R_k\}, \Omega_k) = -\frac{1}{2} + \frac{3}{2} (\hat{\mathbf{n}}(R_k) \cdot \hat{\mathbf{c}}_k)^2 + \lambda \sqrt{\frac{3}{2}} \left[(\hat{\mathbf{n}}(R_k) \cdot \hat{\mathbf{a}}_k)^2 - (\hat{\mathbf{n}}(R_k) \cdot \hat{\mathbf{b}}_k)^2 \right], \quad (13)$$

$$q_2(\{R_k\}, \Omega_k) = \frac{\sqrt{3}}{2} \left[(\hat{\mathbf{l}}(R_k) \cdot \hat{\mathbf{c}}_k)^2 - (\hat{\mathbf{m}}(R_k) \cdot \hat{\mathbf{c}}_k)^2 \right] + \lambda \sqrt{2} \left[(\hat{\mathbf{l}}(R_k) \cdot \hat{\mathbf{a}}_k)^2 + (\hat{\mathbf{m}}(R_k) \cdot \hat{\mathbf{b}}_k)^2 - \frac{1}{2} (\hat{\mathbf{n}}(R_k) \cdot \hat{\mathbf{c}}_k)^2 - \frac{1}{2} \right], \quad (14)$$

and where symbol $\{R_k\} \stackrel{\text{def}}{=} \{\hat{\mathbf{n}}(R_k), \hat{\mathbf{m}}(R_k), \hat{\mathbf{l}}(R_k)\}$ stands for the right-handed tripod of directors ($k = A, B$).

Before going further it seems appropriate to discuss similarities and differences between the present model (8) and that of GLF. To this end we rewrite the GLF Hamiltonian in our notation:

$$H_{\text{MF}}^{\text{GLF}} = -\varepsilon \text{Tr}[\mathbf{Q}_{\text{U}}(\hat{\mathbf{c}}_A) \cdot \bar{\mathbf{Q}}_{\text{U}}(R_A) + \mathbf{Q}_{\text{U}}(\hat{\mathbf{c}}_B) \cdot \bar{\mathbf{Q}}_{\text{U}}(R_B)]. \quad (15)$$

The form of $\bar{\mathbf{Q}}_{\text{U}}$ and $\bar{\mathbf{Q}}$ tensors accounts in both models for the global D_{∞} symmetry point group of the N_{TB} phase with the (optical) C_{∞} axis parallel to the helix axis^{11,42}. N_{TB} is also invariant for the twofold rotation around a local vector $\hat{\mathbf{m}}$, where $\hat{\mathbf{m}}$ is perpendicular to the plane containing the helix axis $\hat{\mathbf{z}}$ and the local director. This local C_2 symmetry causes that N_{TB} is locally polar. As $\hat{\mathbf{n}}$, $\hat{\mathbf{m}}$ and \mathbf{k} are linearly independent the structure is also locally biaxial.

The difference between the two models lies in primary order parameters entering heliconical variational *ansatz* (7) on the N_{TB} structure. While in the GLF model the conical twist-bend helix $\bar{\mathbf{Q}}_{\text{U}}$ is approximated by a locally uniaxial distortion of the director field weighted by q_0 , our $\bar{\mathbf{Q}}$ tensor comprises full set of the directors (1–3) which, along with the variational parameters q_0 and q_2 , permits the helix to be locally biaxial. Both order parameters, q_0 and q_2 , can be determined experimentally along the effective optical axis $\mathbf{k} \parallel \langle \hat{\mathbf{n}} \rangle_p$ ^{16,17,19}, which is an eigenvector of $\langle \bar{\mathbf{Q}} \rangle_p$, where $\langle \dots \rangle_p$ denotes average over one period p along \mathbf{k} . Indeed, the averaged alignment tensor $\langle \bar{\mathbf{Q}} \rangle_p$ is diagonal, uniaxial and of zero trace, and the eigenvector $\langle \hat{\mathbf{n}} \rangle_p$ corresponds to the non-degenerate eigenvalue Λ_k , given by a linear combination of q_0 and q_2 :

$$\Lambda_k = \frac{q_0(3 \cos(2\theta) + 1)}{2\sqrt{6}} + \frac{q_2 \sin^2(\theta)}{\sqrt{2}}. \quad (16)$$

Our extension is also important as it obeys two nematic phases, uniaxial and biaxial, both recovered for pitch $p \rightarrow \infty$, while in the GLF model only a uniaxial nematic phase is present. Further difference between the models concerns the treatment of molecular biaxiality, which we discuss below.

2.3 Effective molecular shape in the nematic limit

V-shaped molecules of both models are biaxial due to their C_{2v} symmetry. In the GLF model they are represented by two uniaxial arms with the bend angle χ , while our model permits molecular arms to be biaxial, with arm's biaxiality controlled by λ . Clearly, in both cases the total molecule is biaxial, but the model (8) allows for full control of a composite molecular biaxiality. In order to illustrate this, we study the effective molecular shape of the two models as seen in the nematic limit ($\phi = 0$ in equations (1–3)). Since in this limit directors become positionally independent, it implies that $\bar{\mathbf{Q}}(R_A) = \bar{\mathbf{Q}}(R_B) \stackrel{\text{def}}{=} \bar{\mathbf{Q}}$ and

$$H_{\text{MF},\text{N}}(\Omega) = -\varepsilon \text{Tr}[(\mathbf{Q}(\Omega_A) + \mathbf{Q}(\Omega_B)) \cdot \bar{\mathbf{Q}}]. \quad (17)$$

That is, with the nematic *ansatz* the segmental mean-field model (8) can be mapped into single site, mean-field version of the dispersion model³⁹, where the bent-shaped molecule is represented by an effective molecular quadrupolar tensor

$$\mathbf{Q}_{\text{mol}} \stackrel{\text{def}}{=} \mathbf{Q}(\Omega_A) + \mathbf{Q}(\Omega_B). \quad (18)$$

The \mathbf{Q}_{mol} tensor is biaxial, also for the GLF model of $\lambda = 0$. The biaxiality of \mathbf{Q}_{mol} can be quantified by calculating the invariant, normalized biaxiality parameter $w = \sqrt{6} \text{Tr}[\mathbf{Q}_{\text{mol}}^3] / \text{Tr}[\mathbf{Q}_{\text{mol}}^2]^{3/2}$ ($w^2 \leq 1$)^{39,41}. It reads

$$w = \frac{3\sqrt{6}(2\lambda^2 + 1)\lambda \sin^2(\chi) + (9 - 30\lambda^2)\cos^2(\chi) - 18\lambda^2 - 1}{(\lambda^2 \cos(2\chi) + 7\lambda^2 - 2\sqrt{6}\lambda \sin^2(\chi) + 3\cos^2(\chi) + 1)^{3/2}}. \quad (19)$$

For the uniaxial states $w^2 = 1$, whereas nonzero biaxiality is monitored by $w^2 < 1$ approaching maximal value for $w = 0$. The case $w > 0$ ($w < 0$) corresponds to prolate (oblate) states of \mathbf{Q}_{mol} . The variation of w with the angle between the two arms calculated from Eq. (19) for a selection of the values of the λ parameter is given in Figure 2.

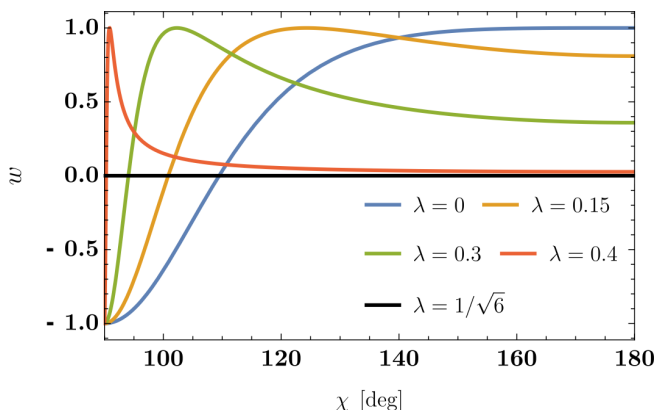


Fig. 2 (Color online) Molecular biaxiality parameter (19) in nematic phase as a function of bend angle for λ equal to: 0 (blue), 0.15 (orange), 0.3 (green), 0.4 (red) and $1/\sqrt{6}$ (black).

For the GLF model ($\lambda = 0$) the V-shaped molecule exhibits effectively disc-like uniaxial shape at $\chi = 90^\circ$, which evolves to rod-like uniaxial one at $\chi = 180^\circ$. The curve in (w, χ) plane passes through zero, the point of maximal molecular biaxiality, when the bend angle is equal to the tetrahedral value ($\chi = \arccos(-1/3) \cong 109.47^\circ$). In spite of this molecular biaxiality the GLF *ansatz* (15) permits only uniaxial structures, which excludes e.g. the biaxial nematic phase.

For $\lambda > 0$ the effective molecular biaxiality can be made less dependent on χ and already for $\lambda \gtrsim 0.15$ the arm-induced biaxiality starts prevailing over. In the limit of maximally biaxial arms ($\lambda = 1/\sqrt{6}$), the effective molecule becomes maximally biaxial irrespective of the angle between the arms. Hence, the simple mean-field model (8) with only two molecular parameters, λ and χ , allows to control almost independently molecular anisotropy and the angle between the arms. They both seem primary to liquid crystal behavior of bent-core, dimeric and trimeric mesogens, especially in view that compounds composed of these molecules are also candidates to exhibit the elusive biaxial nematic phase.

3 Results

In what goes after, we use the following notation for phases: N_U for the uniaxial nematic, N_B for the biaxial nematic, N_{TB} for the twist-bend nematic with heliconical uniaxial *ansatz* ($\bar{\mathbf{Q}}_U$), $N_{TB,B}$

for the twist-bend nematic with heliconical biaxial *ansatz* ($\bar{\mathbf{Q}}$) and Iso for the isotropic phase.

Phase diagrams for banana-shaped biaxial molecules for three typical values: 130° , 135° and 140° of the bend angle χ are presented in Figure 3. For $\chi = 130^\circ$ three phases: N_{TB} , $N_{TB,B}$, and Iso become stable for λ ranging from 0 to the so-called self-dual point³⁹, where $\lambda = 1/\sqrt{6}$. In Figure 3a the $N_{TB,B}$ phase becomes stable below the uniaxial N_{TB} with phase sequence: Iso \rightarrow N_{TB} \rightarrow $N_{TB,B}$, or directly below Iso through sequence: Iso \rightarrow $N_{TB,B}$. Widening the bend angle (see Figures 3b and 3c) leads to stable regions of N_U and even N_B phases, although N_B is visible only in a very narrow region of λ (in the closest vicinity of the self-dual point) and for $\chi = 140^\circ$. Apart from phase transitions that are present for $\chi = 130^\circ$ we can identify the following sequences: Iso \rightarrow N_U \rightarrow N_{TB} \rightarrow $N_{TB,B}$, Iso \rightarrow N_U \rightarrow N_B \rightarrow $N_{TB,B}$ and Iso \rightarrow N_B \rightarrow $N_{TB,B}$. Broadening of regions of the nematic phases, both uniaxial and biaxial, starts with further widening of the bend angle ($\chi > 140^\circ$), where the more ordered twist-bend nematics are moved to lower temperatures, similar to the tetrahedral nematic phases^{43–45}. Interestingly, for $\chi \lesssim 140^\circ$ the nematic twist-bend nematic phase is always more stable than N_B .

In order to better understand the identified phases, we have analyzed temperature variations of uniaxial (q_0) and biaxial (q_2) order parameters, tilt angle (θ) and pitch (p) for the selected cases. Additionally, we have calculated the order parameter $\langle \hat{\mathbf{w}} \cdot \hat{\mathbf{m}}(z = R_C) \rangle$, which gives signature of polar order in the system, and hence allows to identify a nematic twist-bend phases. Figure 4 shows exemplary results for the Iso \rightarrow $N_{TB,B}$ phase sequence, where discontinuity in all parameters indicates on the first order phase transition between these phases. The tilt angle in N_{TB} tends to $\theta = 25^\circ$ and pitch is almost constant, smaller than the length of a stretched molecule.

These results are very close to the exact value for θ that can be obtained for the ground state ($t^* = 0$):

$$\theta(t^* = 0) = \frac{1}{2}(180^\circ - \chi). \quad (20)$$

Indeed, substitution of $\chi = 130^\circ$ gives 25° for θ in this limit. The relation (20), being valid for arbitrary bend angle χ , is also regained for θ in the bottom panel of Figure 5. As concerning pitch of the twist-bend phase it should never exceed $4L$ in the ground state, but can be larger than this value for high temperatures. This is illustrated in Figure 5, where pitch becomes divergent in the vicinity of $N_{TB} \leftrightarrow N_U$ phase transition.

The phase diagram (Figure 3c) is especially rich in sequence of phase transitions. More specifically, we can identify first order phase transitions between $N_{TB,B}$ and N_{TB} and between N_U and Iso phases with discontinuity in order parameters (Figure 5), and second order phase transition between N_{TB} and N_U . The second-order nature of the $N_{TB} \leftrightarrow N_U$ transition can be recognized from temperature variations of conical angle and pitch, where the first goes continuously to zero while the latter diverges at the transition point. We also calculate mean values of uniaxial ($\langle q_0^k \rangle$) and biaxial ($\langle q_2^k \rangle$) order parameters with respect to the optical axis ($\hat{\mathbf{k}} = \mathbf{k}/k$) reference frame: $\{R_{\hat{\mathbf{k}}}\} \stackrel{\text{def}}{=} \{\hat{\mathbf{k}}, \hat{\mathbf{m}}(z = R_C), \hat{\mathbf{k}} \times \hat{\mathbf{m}}(z = R_C)\}$.

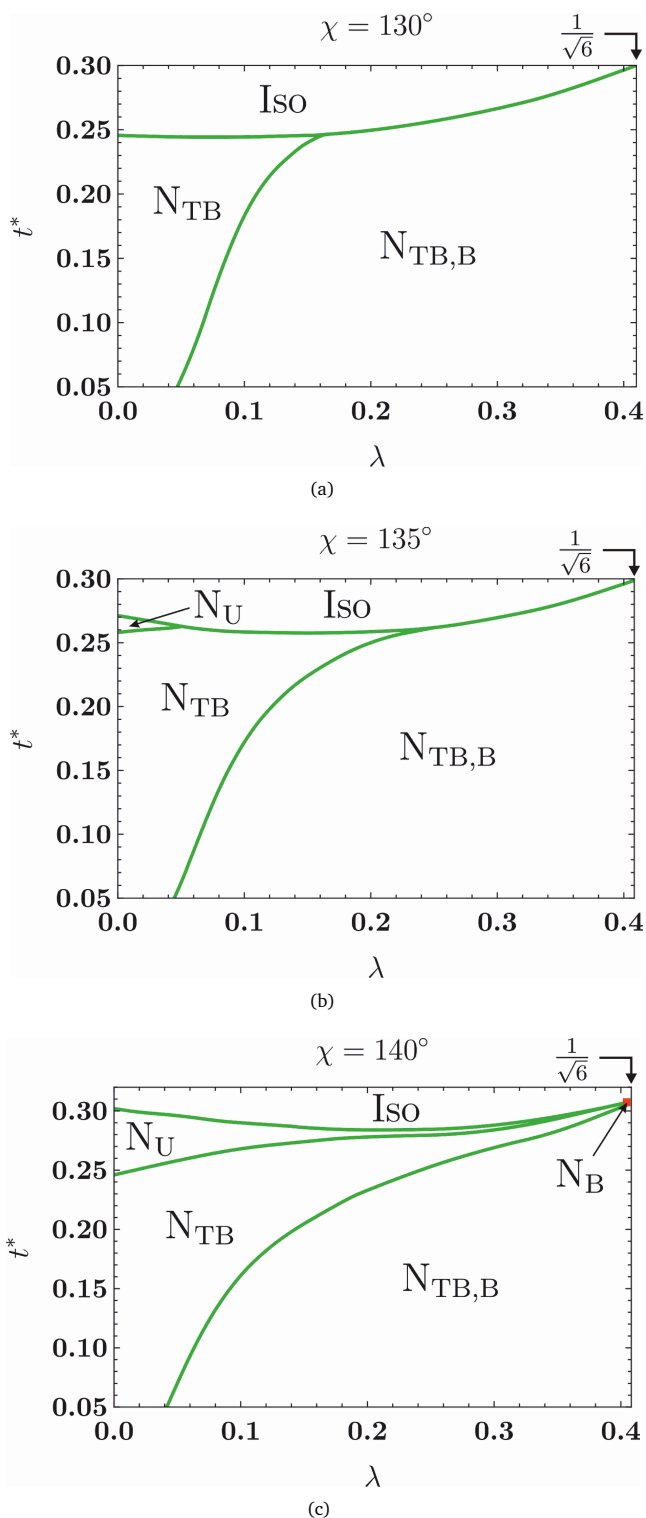


Fig. 3 (Color online) Phase diagrams on (λ, t^*) plane for bend angle equal to (a) 130° , (b) 135° and (c) 140° . Red square in panel (c) represents tiny region where stable N_B phase occurs; its area enhances with further increase of the bending angle χ .

The following averages need to be determined:

$$\langle q_n^k \rangle = \frac{1}{2} \langle q_n(\{\mathbf{R}_{\hat{\mathbf{k}}}\}, \Omega_A) + q_n(\{\mathbf{R}_{\hat{\mathbf{k}}}\}, \Omega_B) \rangle, \quad n = 0, 2. \quad (21)$$

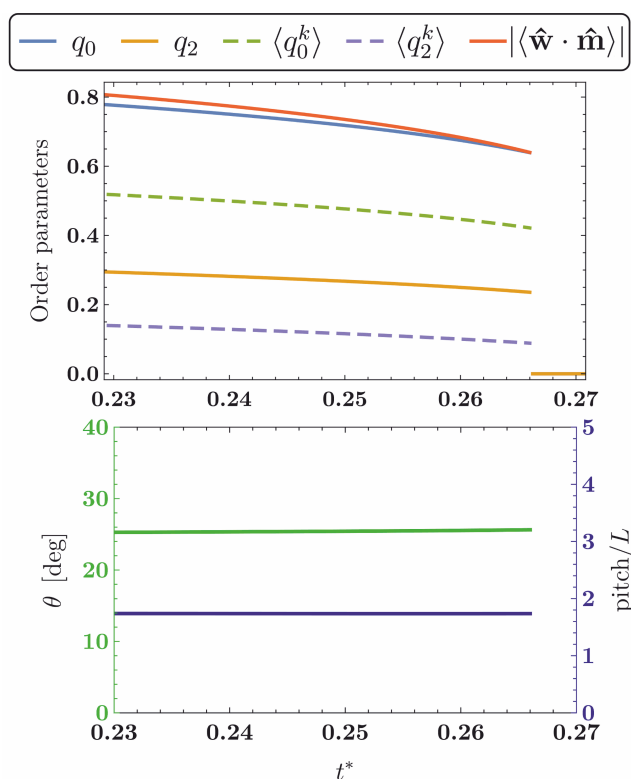


Fig. 4 (Color online) Behavior of order parameters, tilt angle and pitch for phase transition $Iso \rightarrow N_{TB,B}$ when $\lambda = 0.3$ and $\chi = 130^\circ$. q_0 and q_2 are obtained by direct minimization of the free energy (9), $\langle q_0^k \rangle$ and $\langle q_2^k \rangle$ are uniaxial and biaxial order parameters calculated with respect to the wave vector \mathbf{k} , and $|\langle \hat{\mathbf{w}} \cdot \hat{\mathbf{m}} \rangle| \stackrel{\text{def}}{=} |\langle \hat{\mathbf{w}} \cdot \hat{\mathbf{m}}(z = R_C) \rangle|$ is the modulus of polar order parameter.

In the homogeneous N_U phase we expect $\langle q_0^k \rangle = q_0$, which should hold for any non-tilted phase^{46–48}. The same relation is fulfilled by the mean value of biaxial order parameters q_2 and $\langle q_2^k \rangle$ in the N_B phase. Note, however, discrepancies between the order parameters of twist-bend phases calculated in various reference frames. Locally in the arm reference frames q_2 is zero in the N_{TB} phase, while in the $\hat{\mathbf{k}}$ -frame both $\langle q_0^k \rangle$ and $\langle q_2^k \rangle$ are nonzero for any twist-bend phase.

Further examples of phase sequences are presented in Figures 6–8, where $N_B \leftrightarrow N_{TB,B}$ phase transition is of first order, while $N_U \leftrightarrow N_B$ and $Iso \leftrightarrow N_B$ are of second order^{39–41,43–46,49,50}. Interestingly, the conical angle and the pitch in N_{TB} are *ca.* 1.3 to 1.5 and 0.8 to 2.5 times larger, respectively, than those in $N_{TB,B}$ (see Figure 5 and Figure 6). Both twist-bend nematic phases are strongly polar, however favorably more polar is the $N_{TB,B}$ phase. Additionally, it is also noticeable that depending on the value of bending angle χ and biaxiality parameter λ the transition between $N_{TB,B} \leftrightarrow N_{TB}$ may be characterized by significant (Figure 5) or slight (Figure 6) decrease in values of polar order parameter.

Figure 7 shows a magnification of the phase sequence for $\chi = 140^\circ$ in the proximity of the self-dual point (red square in Figure 3c). A noticeable feature of this region is high biaxiality of molecular arms. Though the biaxial phases play a dominant role here, in a small temperature interval, in addition to N_B and $N_{TB,B}$

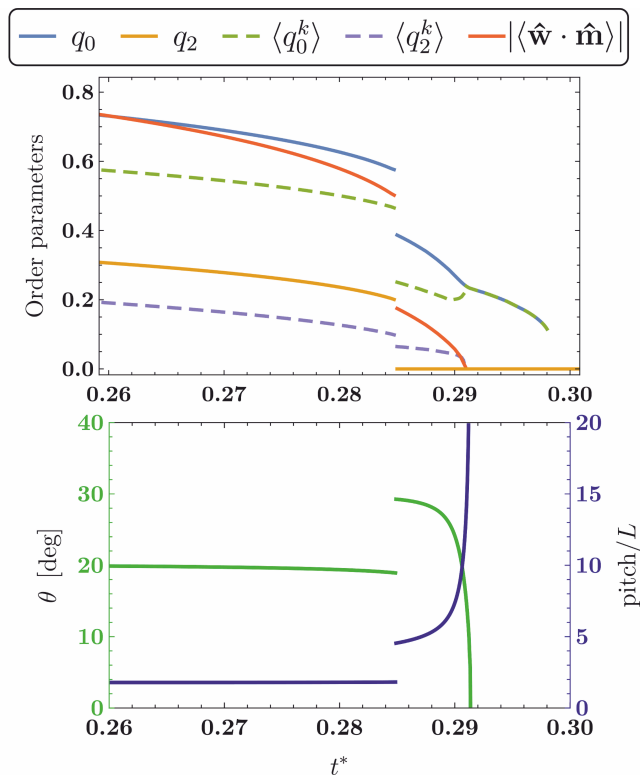


Fig. 5 (Color online) Behavior of order parameters, tilt angle and pitch for Iso \rightarrow N_U \rightarrow N_{TB} \rightarrow $N_{TB,B}$ phase transitions when $\lambda = 0.36$ and $\chi = 140^\circ$. For further details see caption to Figure 4.

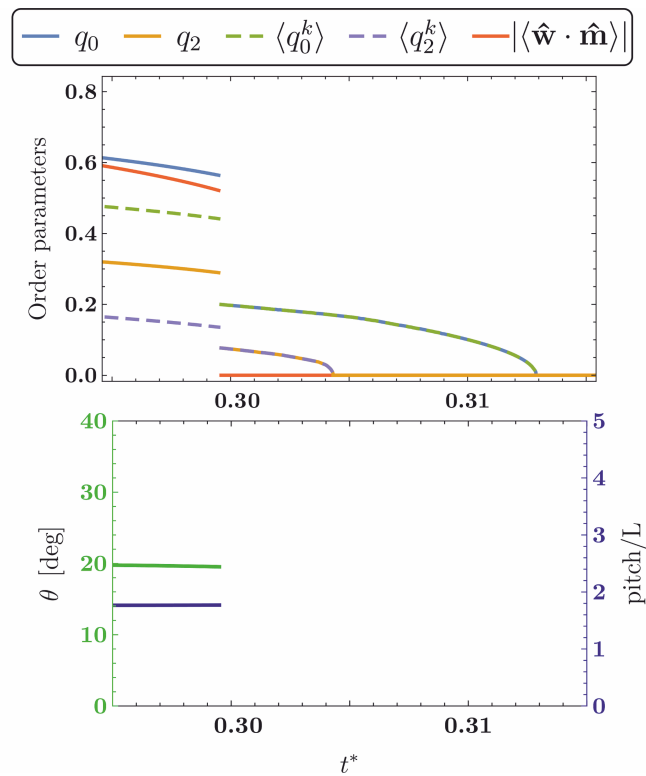


Fig. 7 (Color online) Behavior of order parameters, tilt angle and pitch for the sequence of phase transitions Iso \rightarrow N_U \rightarrow N_B \rightarrow $N_{TB,B}$ when $\lambda = 0.408$ and $\chi = 140^\circ$. For further details see caption to Figure 4.

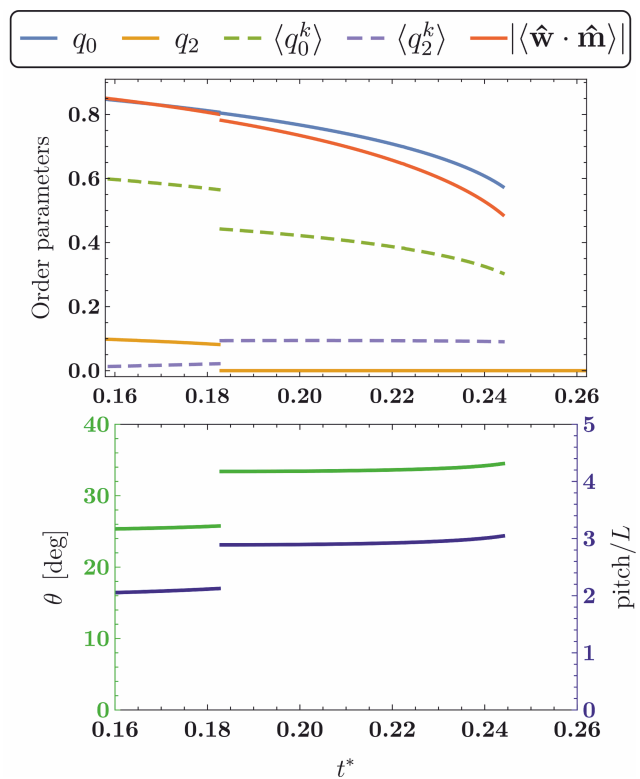


Fig. 6 (Color online) Behavior of order parameters, tilt angle and pitch for phase transitions Iso \rightarrow N_{TB} \rightarrow $N_{TB,B}$ when $\lambda = 0.1$ and $\chi = 130^\circ$. For further details see caption to Figure 4.

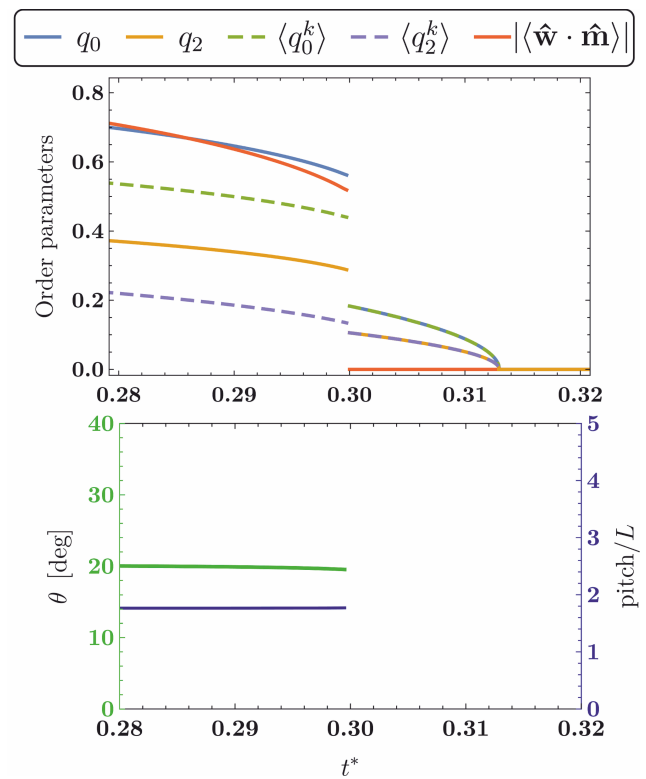


Fig. 8 (Color online) Behavior of order parameters, tilt angle and pitch for the successive phase transitions: Iso \rightarrow N_B \rightarrow $N_{TB,B}$ when $\lambda = 1/\sqrt{6}$ and $\chi = 140^\circ$. For further details see caption to Figure 4.

phases, it is possible to stabilize the N_U phase, as well. The last plot (Figure 8) depicts a phase transition between N_B and $N_{TB,B}$ at the self-dual point ($\lambda = 1/\sqrt{6}$) for the arms and $\chi = 140^\circ$. Here bent-core molecular arms are maximally biaxial (*i.e.* they are neither prolate nor oblate). The $N_B \leftrightarrow N_{TB,B}$ phase transition is first order as can be deduced from a discontinuity in all order parameters (see Figures 7 and 8).

4 Summary

In conclusion, we analyzed an extension of the generic GLF mean-field model¹ to study the role of biaxiality of V-shaped molecules can play in the stabilization of N_{TB} relative to the nematic and isotropic phases. We assumed that each of the two arms of a bent-shaped molecule is intrinsically biaxial and took local biaxial *ansatz* for the alignment tensor. In the limit of uniaxial particles ($\chi = 0^\circ, 180^\circ$ and $\lambda = 0$) we recover mean-field results of Maier and Saupé. For ordinary biaxial molecules ($\chi = 0^\circ, 180^\circ$ and $\lambda \neq 0$) the model becomes reduced to mean-field version of the well known Lebwohl-Lasher dispersion model^{39,50}. As all bent-core molecules are biaxial⁵¹ our generalization seems important for it allows to control intrinsic molecular biaxiality (by two molecular features: bend angle and arm anisotropy).

We showed that in our extended model, in addition to N_U and N_{TB} , two extra phases: homogeneous N_B , and periodic $N_{TB,B}$ – the analog of N_{TB} with local biaxial order of molecular arms – can be studied, where N_B appears in a natural way as a limiting case of $N_{TB,B}$. For small bend angles the phase diagram becomes dominated by the $N_{TB,B}$ phase with no homogeneous nematics present, even for a relatively small molecular biaxiality ($\lambda \lesssim 0.18$). Here, both of the twist-bend structures are reachable directly from the isotropic phase, like in the recently reported experiments^{15,52}. Widening the bend angle opens the path for stabilization of standard nematics, where they start to dominate over less conventional phases as in^{43–45}. However, the stable N_B phase is not found for $\chi \lesssim 140^\circ$.

One can see from Figures 4–8 that the asymptotic relation for the tilt angle (20) is actually the limit for θ in the $N_{TB,B}$ phase, as this structure is a ground state for $0 < \lambda \leq 1/\sqrt{6}$. At the transition between the two twist-bend nematics both the pitch and the cone angle in $N_{TB,B}$ are smaller than in the N_{TB} phase.

Finally, the model introduced in this paper can be extended further to include competition between such molecular/external factors as (steric/electric) dipolar forces and external field(s)^{46,53,54}. Then, further nematic structures with one-dimensional modulation are also expected^{24–29,55,56}.

Acknowledgments

This work was supported by Grant No. DEC-2013/11/B/ST3/04247 of the National Science Centre in Poland and in part by PL-Grid Infrastructure. The authors are grateful to Oleg D. Lavrentovich for pointing out the necessity of improvements in Figure 1 and the authors thank Michał Cieřła and Paweł Karbownik for further stylistic comments and suggestions regarding this Figure. The authors would like to thank the Referees for valuable suggestions in improving the manuscript.

References

- 1 C. Greco, G. R. Luckhurst and A. Ferrarini, *Soft Matter*, 2014, **10**, 9318.
- 2 V. Borshch, Y.-K. Kim, J. Xiang *et al.*, *Nat. Commun.*, 2013, **4**, 1.
- 3 D. Chen, J. H. Porada, J. B. Hooper *et al.*, *Proc. Natl. Acad. Sci. USA*, 2013, **110**, 15931.
- 4 E. Górecka, N. Vaupotič, A. Zep *et al.*, *Angew. Chem. Int. Ed. Engl.*, 2015, **54**, 10155.
- 5 D. Chen, M. Nakata, R. Shao *et al.*, *Phys. Rev. E*, 2014, **89**, 022506.
- 6 M. Cestari, S. Diez-Berart, D. Dunmur *et al.*, *Phys. Rev. E*, 2011, **84**, 031704.
- 7 Y. Wang, G. Singh, D. M. Agra-Kooijman *et al.*, *CrystEngComm*, 2015, **17**, 2778.
- 8 C.-J. Yun, M. R. Vengatesan, J. K. Vij *et al.*, *Appl. Phys. Lett.*, 2015, **106**, 173102.
- 9 R. R. de Almeida, C. Zhang, O. Parri *et al.*, *Liq. Cryst.*, 2014, **41**, 1661.
- 10 N. Sebastián, D. O. Lopez, B. Robles-Hernández *et al.*, *Phys. Chem. Chem. Phys.*, 2014, **16**, 21391.
- 11 C. Meyer, G. R. Luckhurst and I. Dozov, *J. Mater. Chem. C*, 2015, **3**, 318.
- 12 B. Robles-Hernández, N. Sebastián, M. R. de la Fuente *et al.*, *Phys. Rev. E*, 2015, **92**, 062505.
- 13 C. Zhu, M. R. Tuchband, A. Young *et al.*, *Phys. Rev. Lett.*, 2016, **116**, 147803.
- 14 R. J. Mandle, E. J. Davis, C. T. Archbold *et al.*, *Chem. Eur. J.*, 2015, **21**, 8158.
- 15 A. A. Dawood, M. C. Grossel, G. R. Luckhurst *et al.*, *Liquid Crystals*, 2016, **43**, 2.
- 16 E. I. Kats and V. V. Lebedev, *JETP Letters*, 2014, **100**, 110.
- 17 C. Meyer and I. Dozov, *Soft Matter*, 2016, **12**, 574.
- 18 A. G. Vanakaras and D. J. Photinos, *Soft Matter*, 2016, **12**, 2208.
- 19 Z. Parsouzi, S. M. Shamid, V. Borshch *et al.*, *Phys. Rev. X*, 2016, **6**, 021041.
- 20 N. Vaupotič, S. Curk, M. A. Osipov *et al.*, *Phys. Rev. E*, 2016, **93**, 022704.
- 21 G. Barbero, L. R. Evangelista, M. P. Rosseto, R. S. Zola and I. Lelidis, *Phys. Rev. E*, 2015, **92**, 030501.
- 22 C. Greco and A. Ferrarini, *Phys. Rev. Lett.*, 2015, **115**, 147801.
- 23 M. A. Osipov and G. Pająk, *Eur. Phys. J. E*, 2016, **39**, 45.
- 24 L. Longa and G. Pająk, *Phys. Rev. E*, 2016, **93**, 040701.
- 25 R. B. Meyer, *Proceedings of the Les Houches Summer School on Theoretical Physics, 1973, session No. XXV*, New York: Gordon and Breach, 1976.
- 26 R. B. Meyer, *Phys. Rev. Lett.*, 1969, **22**, 918.
- 27 I. Dozov, *Europhys. Lett.*, 2001, **56**, 247.
- 28 V. L. Lorman and B. Mettout, *Phys. Rev. Lett.*, 1999, **82**, 940.
- 29 V. L. Lorman and B. Mettout, *Phys. Rev. E*, 2004, **69**, 061710.
- 30 Z. Ahmed, C. Welch and G. H. Mehl, *RSC Adv.*, 2015, **5**, 93513.

- 31 R. Memmer, *Liq. Cryst.*, 2002, **29**, 483.
- 32 S. M. Shamid, S. Dhakal and J. V. Selinger, *Phys. Rev. E*, 2013, **87**, 052503.
- 33 J. W. Emsley, M. Lelli, A. Lesage *et al.*, *J. Phys. Chem. B*, 2013, **117**, 6547.
- 34 A. Pizzirusso, M. E. Di Pietro, G. De Luca *et al.*, *ChemPhysChem*, 2014, **15**, 1356.
- 35 M. A. Bates and G. R. Luckhurst, *Phys. Rev. E*, 2005, **72**, 051702.
- 36 P. Grzybowski and L. Longa, *Phys. Rev. Lett.*, 2011, **107**, 027802.
- 37 M. A. Osipov and G. Pająk, *J. Phys.: Condens. Matter*, 2012, **24**, 142201.
- 38 T. C. Lubensky and L. Radzihovsky, *Phys. Rev. E*, 2002, **66**, 031704.
- 39 L. Longa, P. Grzybowski, S. Romano *et al.*, *Phys. Rev. E*, 2005, **71**, 051714.
- 40 C. Chiccoli, P. Pasini, F. Semeria *et al.*, *Int. J. Mod. Phys. C*, 1999, **10**, 469.
- 41 L. Longa and G. Pająk, *Liquid Crystals*, 2005, **32**, 1409.
- 42 C. Meyer, G. R. Luckhurst and I. Dozov, *Phys. Rev. Lett.*, 2013, **111**, 067801.
- 43 L. Longa, G. Pająk and T. Wydro, *Phys. Rev. E*, 2009, **79**, 040701.
- 44 L. Longa and G. Pająk, *Mol. Cryst. Liq. Cryst.*, 2011, **541**, 152/[390].
- 45 K. Trojanowski, G. Pająk, L. Longa *et al.*, *Phys. Rev. E*, 2012, **86**, 011704.
- 46 P. G. de Gennes and J. Prost, *The Physics of Liquid Crystals*, Clarendon Press, 2nd edn., 1993.
- 47 G. Pająk and M. A. Osipov, *Phys. Rev. E*, 2013, **88**, 012507.
- 48 M. Osipov and G. Pająk, *Phys. Rev. E*, 2012, **85**, 021701.
- 49 *Biaxial Nematic Liquid Crystals: Theory, Simulation and Experiment*, ed. G. R. Luckhurst and T. J. Sluckin, John Wiley & Sons, Ltd., 2015.
- 50 R. Berardi, L. Muccioli, S. Orlandi *et al.*, *J. Phys.: Condens. Matter*, 2008, **20**, 463101.
- 51 A. Jákli, *Liq. Cryst. Rev.*, 2013, **1**, 65.
- 52 C. T. Archbold, E. J. Davis, R. J. Mandle *et al.*, *Soft Matter*, 2015, **11**, 7547.
- 53 K. Trojanowski, D. W. Allender, L. Longa *et al.*, *Mol. Cryst. Liq. Cryst.*, 2011, **540**, 59.
- 54 R. S. Zola, G. Barbero, I. Lelidis *et al.*, *arXiv:1602.07530*.
- 55 L. Longa and H.-R. Trebin, *Phys. Rev. A*, 1990, **42**, 3453.
- 56 N. Vaupotič, M. Čepič, M. A. Osipov *et al.*, *Phys. Rev. E*, 2014, **89**, 030501.